

Crystallographic Structure Determination of Both [5,6]- and [6,6]-Isomers of Lithium-Ion-Containing Diphenylmethano[60]fullerene

Hiroshi Okada,[†] Hiroki Kawakami,[‡] Shinobu Aoyagi,^{*,§,||} and Yutaka Matsuo^{*,†,||}

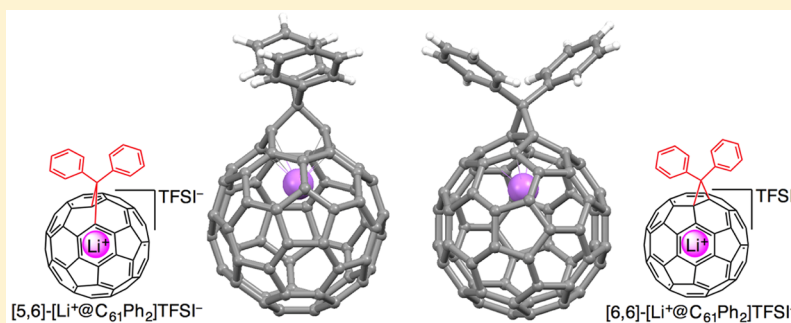
[†]Department of Mechanical Engineering, School of Engineering, The University of Tokyo, 7-3-1 Hongo, Bunkyo-ku, Tokyo 113-8565, Japan

[‡]Department of Chemistry, School of Science, The University of Tokyo, 7-3-1 Hongo, Bunkyo-ku, Tokyo 113-0033, Japan

[§]Department of Information and Basic Science, Nagoya City University, Nagoya 467-8501, Japan

^{||}Hefei National Laboratory for Physical Sciences at Microscale, University of Science and Technology of China, 96 Jinzhai Road, Hefei, Anhui 230026, China

S Supporting Information



ABSTRACT: Organic functionalization of lithium-ion-containing [60]fullerene, $\text{Li}^+\text{@C}_{60}$, was performed by using diphenyl-(diazomethane) as a stable, readily available diazo compound to obtain lithium-ion-containing [5,6]- and [6,6]-diphenylmethano[60]fullerenes, $\text{Li}^+\text{@C}_{61}\text{Ph}_2$. The bis(trifluoromethanesulfonyl)imide (TFSI) salts of [5,6]- and [6,6]- $\text{Li}^+\text{@C}_{61}\text{Ph}_2$ were successfully separated by using a cation exchange column with eluent containing LiTFSI . Improved separation protocol and high crystallinity of ionic components in less polar solvents enabled separate crystallization of each isomer. Both [5,6]-open and [6,6]-closed structures of $\text{Li}^+\text{@C}_{61}\text{Ph}_2$ were determined by synchrotron radiation X-ray crystallography. Elucidating the [5,6]-open methano[60]fullerene (fulleroid) structure will contribute to materials research on fulleroids.

INTRODUCTION

Methano[60]fullerene^{1–6} is one of the most important classes of fullerene derivatives in the materials science and chemistry of fullerenes. It has a simple structure with a compact methano ($:\text{CH}_2$) addend on C_{60} , which can be unsubstituted or can accommodate various substituents. A representative substituted methano[60]fullerene is [6,6]-phenyl- C_{61} -butyric acid methyl ester, PCBM,⁷ which has been widely used as a standard electron acceptor in organic solar cells research.⁸ In addition, unsubstituted methano[60]fullerene (C_{61}H_2)³ derivatives have recently been used to increase the performance of organic⁹ and perovskite¹⁰ solar cells, with the simple methano addend being utilized to realize high electron mobility.

After methano[60]fullerene was first reported by Wudl and colleagues in the early years of fullerene research,¹ the manner in which the methano group is attached to the fullerene cage has been extensively investigated.^{1–5} Four possible configurations can be drawn as shown in Figure 1. In the first report of methano[60]fullerene in 1991,^{1a} a [6,6]-open structure was proposed for the product. In-depth investigation revealed that the first kinetically obtained product is the [5,6]-open

methano[60]fullerene,^{1b} which is called “fulleroid”¹ because of its spectroscopic similarity to C_{60} , and undergoes conversion to the [6,6]-closed form,³ which is a thermodynamically stable product.^{1b,2–5} The [6,6]-closed structure was then characterized by X-ray crystallography.⁶ Thereafter, the structures of many [6,6]-closed methano[60]fullerene derivatives have been unambiguously determined by X-ray analysis. Another isomer, the [5,6]-adduct, is of potential interest in research on structural and physical properties, but its crystal structure has yet to be accurately obtained.¹¹ We attribute this to the difficulty of isolating the [5,6]-isomer, which is a kinetic isomer, in its pure form. The [5,6]-isomer is partly converted to the [6,6]-isomer under ambient light, which causes problems in the purification and crystallization of the [5,6]-isomer. In particular, co-crystallization of these isomers was an obstacle to prior crystallographic analysis of the [5,6]-isomer.¹¹

In this work, we employed lithium-ion-containing [60]-fullerene, $\text{Li}^+\text{@C}_{60}$,¹² to isolate both the [5,6]- and [6,6]-

Received: March 29, 2017

Published: May 10, 2017

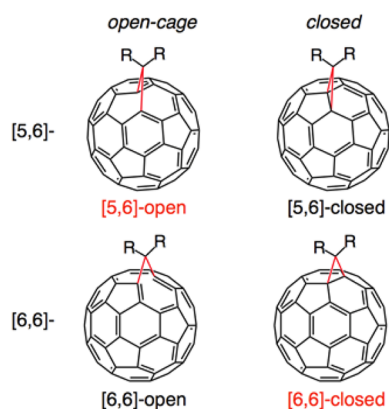


Figure 1. Four possible addition manners of the methano groups attached onto the [60]fullerene cage.

isomers (Figure 2) for X-ray crystallographic analysis. $\text{Li}^+\text{@C}_{60}$ has recently attracted considerable interest in electrochemis-

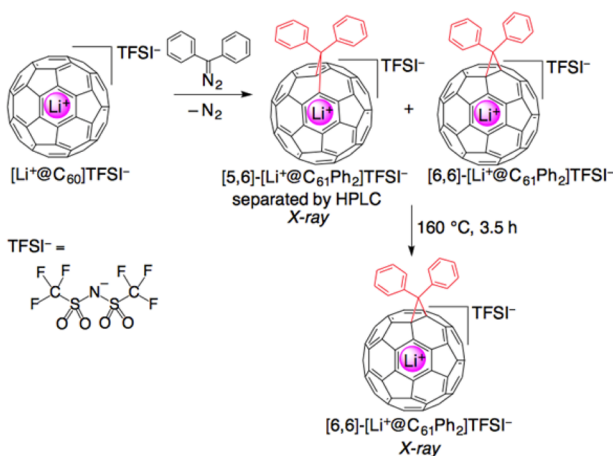


Figure 2. Synthesis of lithium-ion-containing diphenylmethano[60]-fullerenes.

try,¹³ supramolecular chemistry,¹⁴ physics,¹⁵ and organic chemistry.¹⁶ Studies in synthetic chemistry have demonstrated the remarkably high chemical reactivity of $\text{Li}^+\text{@C}_{60}$.^{16b,c} Here we successfully crystallized each isomer separately, avoiding problematic co-crystallization, by utilizing improved separation protocol and high crystallinity of ionic components. Elucidating the [5,6]-open methano[60]fullerene (fulleroid) structure will provide essential information for further basic and applied research of fullerene-based materials.

RESULTS AND DISCUSSION

Synthesis, Purification, and Characterization of [5,6]- and [6,6]-Lithium-Ion-Containing Diphenylmethano[60]fullerenes. To synthesize lithium-ion-containing methano[60]fullerenes, we used diphenyl(diazo)methane (Ph_2CN_2), which is a readily available and stable diazo compound (Figure 2). In general, diazo compounds are not stable, but this compound is stabilized by its adjacent phenyl groups. In addition, we used $\text{Li}^+\text{@C}_{60}$ bis(trifluoromethanesulfonyl)imide (TFSI⁻) salt because of its good solubility. Generally available $[\text{Li}^+\text{@C}_{60}]\text{PF}_6^-$ only partly dissolves in organic solvents as a result of its rock-salt-type packing,^{12c} whereas the TFSI⁻ salt is 10 times more soluble.¹⁷ Reaction of

$[\text{Li}^+\text{@C}_{60}]\text{TFSI}^-$ with 1.1 equiv of Ph_2CN_2 in dichloromethane at room temperature for 5 min produced a reaction mixture containing the target monodiphenylmethano compounds [5,6]- and [6,6]- $[\text{Li}^+\text{@C}_{61}\text{Ph}_2]\text{TFSI}^-$, bisadducts, and unreacted $\text{Li}^+\text{@C}_{60}$ in approximately 45%, 5%, and 50% yield by HPLC area, respectively (Figure 3). The reaction proceeded smoothly,

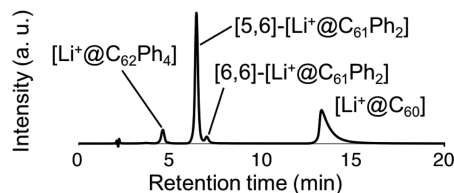


Figure 3. HPLC chart of before and after the reaction for synthesizing $\text{Li}^+\text{@C}_{61}\text{Ph}_2$. Column: InertSil CX (cation exchange column, $\phi 4.6 \times 250$ mm), chlorobenzene:acetonitrile = 1:3 v/v containing 2.5 mM LiTFSI, flow rate: 1.5 mL/min, detector: UV 350 nm.

because nucleophilic addition of 1,3-dipolar compounds (diazo compounds) to C_{60} was facilitated by highly electron-accepting $\text{Li}^+\text{@C}_{60}$.^{16c} Regarding the monoadduct, the [5,6]-adduct dominantly formed over the [6,6]-adduct. This was different from the reaction with empty fullerene to obtain diarylmethano[60]fullerenes, where [5,6]-open and [6,6]-closed isomers were usually obtained in ca. 75:25.¹⁸ We speculate this is due to the high reactivity of $\text{Li}^+\text{@C}_{60}$ over the empty fullerene, selectively giving much [5,6]-open kinetic product. As expected, the retention times of the [5,6]- and [6,6]-monoadducts were close to each other, necessitating development of an appropriate HPLC protocol for separation.

To date, our laboratory has used Buckyprep and π -NAP columns with tetramethylammonium hexafluorophosphate salts added to the eluent for purification of $\text{Li}^+\text{@C}_{60}$ derivatives.^{16a-c} This protocol has enabled successful isolation of $\text{Li}^+\text{@C}_{60}$ derivatives but has some problems. The use of this ammonium salt increases in the column pressure, resulting in low separation efficiency. Moreover, fullerene purification columns are usually very expensive. To solve these problems, we developed a new HPLC protocol for the separation of $\text{Li}^+\text{@C}_{60}$ derivatives, using an inexpensive cation exchange column. We chose LiTFSI as a highly soluble and stable supporting additive to the eluent. LiTFSI dissolves in a mixture of chlorobenzene and acetonitrile, but does not dissolve in chlorobenzene alone. On the other hand, TFSI salts of $\text{Li}^+\text{@C}_{60}$ derivatives have good solubility in chlorobenzene but not in diethyl ether. With these solubility profiles, successful separation was achieved by use of the cation exchange column. After elution of the desired product, acetonitrile was removed by vacuum evaporation to precipitate excess LiTFSI. The concentrated supernatant in chlorobenzene was then poured into diethyl ether to obtain the target product.

Using this protocol, we successfully separated $[\text{Li}^+\text{@C}_{61}\text{Ph}_2]\text{TFSI}^-$ from a mixture of the starting material, monoadducts, and bisadducts. Under preparative separation conditions, the peaks for the [5,6]- and [6,6]-monoadducts still overlapped due to their similar structures (Figure S1). We separately took the earlier fraction containing only [5,6]-product and the later fraction containing both [5,6]- and [6,6]-ones. The latter fraction was subjected to thermal conversion from the [5,6]-isomer to the [6,6]-isomer in *o*-dichlorobenzene at 160 °C for 3.5 h to obtain the pure [6,6]-product.

The purity of isolated [5,6]- and [6,6]-[Li⁺@C₆₁Ph₂]TFSI⁻ was confirmed by analytical HPLC (Figure S2) and ⁷Li NMR (Figure S3). In the ¹H NMR spectra of [5,6]- and [6,6]-[Li⁺@C₆₁Ph₂]TFSI⁻ (Figure S4), signals for the two phenyl groups appeared in asymmetric and symmetric manners, respectively, consistent with the expected structural configurations of these compounds. In their ¹³C NMR spectra (Figure S5), the bridging carbon atoms in [5,6]- and [6,6]-adducts showed signals at 65.21 and 61.04 ppm, respectively, and the fullerene sp² carbons displayed 32 and 17 signals, respectively, in line with their molecular symmetry (C_s and C_{2v} on the NMR time scale). The ⁷Li NMR spectra of the [5,6]- and [6,6]-adducts had signals at -10.6 and -12.6 ppm, respectively, consistent with the lithium ion being more strongly shielded in the [6,6]-methano[60]fullerene cage than in the [5,6]-cage.^{16a,19} This can be explained with considering the number and effect of five- and six-membered rings of fullerenes. While π-electron conjugated systems in the [5,6]-open fullerenes are not largely affected by chemical modification, [6,6]-closed fullerenes lose two diatropic hexagons and two paratropic pentagons. Nucleus-independent chemical shift calculation²⁰ of hexagon and pentagon of C₆₀ has told us that hexagon and pentagon contribute to upfield and downfield shifts, respectively, and effect of one pentagon is larger than that of one hexagon, as one can image from the fact that C₆₀ has 12 pentagons and 20 hexagons. The [6,6]-closed fullerene is affected by loss of two pentagons rather than loss of two hexagons, and accordingly the inner Li⁺ signal is shifted to upfield. MALDI-Fourier transform ion cyclotron resonance mass spectra of the [5,6]- and [6,6]-adducts exhibited parent ion peaks for their cationic parts (Figure S6).

UV-vis absorption spectra (Figure S7) showed broad absorption in the visible range with absorption maxima at 546 and 503 nm for the [5,6]- and [6,6]-monoadducts, respectively. These absorption patterns correspond to those for [5,6]-fulleroid and [6,6]-methanofullerenes,^{3a} and the [5,6]- and [6,6]-Li⁺@C₆₁Ph₂ solutions were purple and orange, respectively. In cyclic voltammograms (Figure S8), [5,6]- and [6,6]-Li⁺@C₆₁Ph₂ exhibited first reduction potentials at -0.40 and -0.49 V, respectively, vs Fc/Fc⁺ (Table S1).

UV-vis absorption spectra (Figure S7) showed broad absorption in the visible range with absorption maxima at 546 and 503 nm for the [5,6]- and [6,6]-monoadducts, respectively. These absorption patterns correspond to those for [5,6]-fulleroid and [6,6]-methanofullerenes,^{3a} and the [5,6]- and [6,6]-Li⁺@C₆₁Ph₂ solutions were purple and orange, respectively. In cyclic voltammograms (Figure S8), [5,6]- and [6,6]-Li⁺@C₆₁Ph₂ exhibited first reduction potentials at -0.40 and -0.49 V, respectively, vs Fc/Fc⁺ (Table S1).

Crystallographic Characterization of Both [5,6]- and [6,6]- Lithium-Ion-Containing Diphenylmethano[60]-fullerenes. Single crystals for both [5,6]- and [6,6]-isomers were successfully obtained. In general, ionic compounds have high crystallinity in less polar solvents, because of the electrostatic interaction between their cationic and anionic parts. Thus, we grew the single crystals of the [5,6]- and [6,6]-isomers from chlorobenzene/diethyl ether and *o*-dichlorobenzene/diethyl ether solutions, respectively.

The crystal structures of [5,6]- and [6,6]-[Li⁺@C₆₁Ph₂]TFSI⁻ at 100 K were determined by synchrotron radiation X-ray structural analysis (Figures 4 and S9; Table S3). Iversen et al. previously attempted X-ray structure analysis of a [5,6]-methano[60]fullerene, [5,6]-C₆₁Ar₂ (Ar = 4-BrC₆H₄).¹¹ However, the crystal was a twinned co-crystal involving both [6,6]- and [5,6]-isomers, with the latter as the minor component. Consequently, accurate structure data for the [5,6]-isomer could not be obtained. Here, we were able to obtain [5,6]-open methano[60]fullerene (fulleroid) as a pure, single crystal and accurately elucidated its structure for the first time. The C1–C2 and C1–C3 bond lengths were both 1.51 Å, slightly shorter than the normal C(sp³)–C(sp³) bond length of 1.54 Å. The distance between the C2 and C3 atoms was 2.13 Å. This value

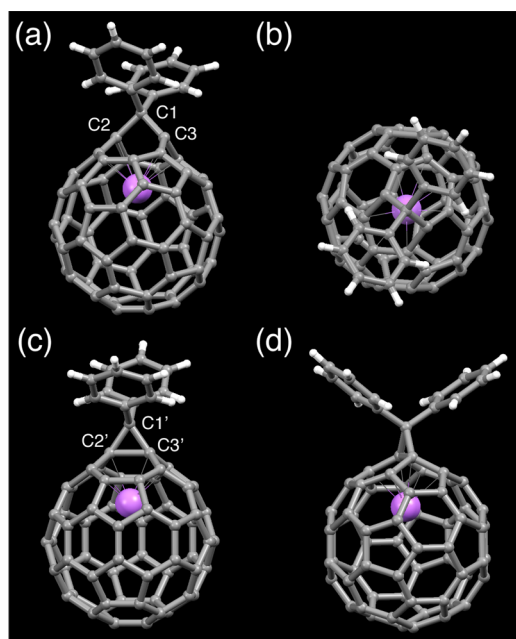


Figure 4. X-ray crystal structures. (a and b) [5,6]-[Li⁺@C₆₁Ph₂]TFSI⁻-(chlorobenzene). (c and d) [6,6]-[Li⁺@C₆₁Ph₂]TFSI⁻-(*o*-dichlorobenzene). Only cationic parts are shown. The interatomic distances between Li⁺ and the C2 (C2') and C3 (C3') carbon atoms are 2.39 (2.30) and 2.38 (2.30) Å, respectively.

is comparable to that found in the [5,6]-open cage structure of C₇₀ and an endohedral metallofullerene with a higher fullerene cage.²¹ Other bond distances around C2 and C3 are shown in Figure 5 (and Figure S10), indicating normal single-bond and double-bond character.

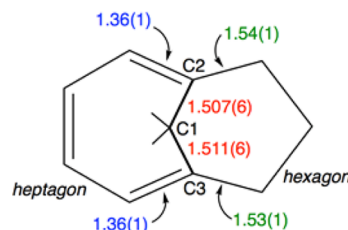


Figure 5. Bond distances (Å) around the C2 and C3 carbon atoms in [5,6]-Li⁺@C₆₁Ph₂. More information is available in Figure S10.

The crystal structure of the [6,6]-isomer revealed a unique feature of the inner Li⁺ ion. First, the well-known three-membered ring was seen (Figure 4c). The C1'–C2' and C1'–C3' bond lengths were both 1.51 Å, which are comparable to those in the [5,6]-isomer. The C2'–C3' bond length was 1.70 Å, which is markedly longer than the bond lengths reported for empty [6,6]-methano[60]fullerenes (Table S2). The DFT calculation (Gaussian09, B3LYP/6-31G(d)) also showed a 0.04 Å longer C2'–C3' bond length in the Li⁺-containing [6,6]-C₆₁Ph₂ (1.653 Å) than the empty one (1.613 Å) (Figure S11). We ascribe this unusually long bond to internal coordination of Li⁺ to the C2'–C3' bond, partially forming a three-center two-electron bond involving these three atoms.

Both [5,6]- and [6,6]-[Li⁺@C₆₁Ph₂]TFSI⁻ crystals had similar molecular packing structures. Close inspection of the packing structures of the two isomers revealed a slightly different direction of the phenyl groups (Figure S9). We

attribute this slight difference to the effect of counteranions on the direction of the $\text{Li}^+@C_{61}\text{Ph}_2$ cationic part through electrostatic interaction.^{12a} In addition, because of existence of counteranions, the [5,6]-isomer can only form a triclinic crystal system ($P\bar{1}$) due to the lower molecular symmetry (C_s) and cannot form higher symmetric crystal system even with disordering atomic positions. This crystal system is different from that of the [6,6]-isomer (monoclinic, $C2/m$ with the C_{2v} molecular symmetry). Thus, crystal packing structures were similar but different from each other. In addition to high crystallinity, the ionic structure was advantageous in obtaining each isomer as a pure, single crystal and avoiding problems with twinning.¹¹

Relative Gibbs energies of the [5,6]-isomer vs the [6,6]-isomer were computationally estimated with DFT calculation (Figure S11, Table S4).⁵ [5,6]- $\text{Li}^+@C_{61}\text{Ph}_2$ had 8.05 kcal/mol higher Gibbs energy than [6,6]- $\text{Li}^+@C_{61}\text{Ph}_2$. As for the empty structures, relative Gibbs energy for [5,6]- $C_{61}\text{Ph}_2$ was calculated to be 9.36 kcal/mol against [6,6]- $C_{61}\text{Ph}_2$. Smaller relative Gibbs energy for the Li^+ -containing one suggests that the [5,6]-adduct is relatively stabilized by the encapsulated Li^+ . This is also advantageous for determination of the crystal structure of the [5,6]-isomer.

The successful crystal structure analysis of both [5,6]- and [6,6]-isomers will offer helpful clues for further understanding the mechanism by which the [5,6]-isomer is converted to the [6,6]-isomer.^{3b,5,16a,22} Materials research on [5,6]-fulleroid will be facilitated by accurate structural information, which has been much scarcer than that available for [6,6]-methano[60]-fullerenes. Physical research focused on localization or motion of the encapsulated Li^+ inside the C_{60} cage will be an interesting research subject.¹⁵

CONCLUSION

In summary, the structures of both [5,6]- and [6,6]-methano[60]fullerene were unambiguously determined by crystallographic analysis. Of note, an accurate crystal structure of [5,6]-methano[60]fullerene (fulleroid) was revealed for the first time by employing a counteranion which enabled easy crystallization and gave different crystal system, thereby avoiding undesired co-crystallization. In addition, the purification method reported here does not require the use of expensive fullerene purification columns and can be put to practical use in this area of research. Furthermore, among the organically functionalized $\text{Li}^+@C_{60}$ derivatives that we have previously synthesized to date,^{16a-c} the present reaction with diphenyl(diazo)methane serves as the easiest chemical modification of $\text{Li}^+@C_{60}$ because of stability of this diazo compound. Considering the important role of chemically modified fullerenes,²³ this compound will contribute to accelerating interdisciplinary research on $\text{Li}^+@C_{60}$.

EXPERIMENTAL SECTION

General. ^1H and ^{13}C NMR spectra were recorded on a JEOL ECA-600. ^7Li NMR spectra were recorded on a JEOL ECX-400 and referenced externally to LiCl in D_2O . The mass spectra were acquired by high-resolution mass spectra, which were obtained by matrix-assisted laser desorption/ionization (MALDI) using a Fourier transform ion cyclotron resonance (FT-ICR) mass analyzer on Bruker solariX 9.4T spectrometer. A starting material, $[\text{Li}^+@C_{60}]\text{PF}_6^-$, was supplied from a commercial supplier. Other chemicals were purchased from other commercial suppliers and used as received.

Preparation of Diphenyldiazomethane. Preparation of diphenyl-diazomethane was referred to the literature method.²⁴ To

water-cooled ether (5 mL) were added benzophenone hydrazone ($\text{Ph}_2\text{C}=\text{NNH}_2$) (300 mg, 1.53 mmol), Ag_2O (355 mg, 1.53 mmol), and MgSO_4 (100 mg, 0.83 mmol), and the mixture was stirred for 30 min keeping the temperature around 30–32 °C. The solution was filtered and evaporated. The residue was dissolved in hexane, subjected to alumina short-pass column (3 cm), and evaporated. Resulted reddish purple solid was used for the reaction below without further purification. The solid could be stored in a freezer for several months.

Procedures for the Synthesis of $[\text{Li}^+@C_{61}\text{Ph}_2]\text{TFSI}^-$. The above-mentioned diphenyldiazomethane (16.9 mg) was dissolved in dichloromethane (5.0 mL). To dichloromethane solution (3.0 mL) of $[\text{Li}^+@C_{60}]\text{TFSI}^-$ (9.3 mg, 9.2 μmol) cooled in EtOH/dry ice bath was slowly added the diphenyldiazomethane solution (583 μL , 1.97 mg, 10.1 μmol). Then, the solution was concentrated in vacuo. Purification of the product was performed by HPLC using an ion exchange column (column: Inertsil CX, $\phi 10 \times 250$ mm, GL Science; flow rate: 7.0 mL/min; eluent: (A) chlorobenzene:acetonitrile = 1:1 v/v with 10 mM LiTFSI , (B) acetonitrile with 10 mM LiTFSI ; gradient: A/B = 35/65 to 70/30 (5–10 min), A/B = 70/30 (after 10 min)). The peak corresponding to monoadducts was collected separately by almost half and half (Figure S1). For the collected fractions, solvent was evaporated in vacuo. When almost all of the acetonitrile was removed, LiTFSI was precipitated. The solutions were concentrated and filtered. Recrystallization by vapor diffusion of diethyl ether afforded pure [5,6]- $[\text{Li}^+@C_{61}\text{Ph}_2]\text{TFSI}^-$ (1.5 mg, 14% yield) from former fraction and mixture of [5,6]- and [6,6]- $[\text{Li}^+@C_{61}\text{Ph}_2]\text{TFSI}^-$ (0.7 mg, 6% yield) from later fraction. Spectral data for [5,6]- $[\text{Li}^+@C_{61}\text{Ph}_2]\text{TFSI}^-$: ^1H NMR (600 MHz, 1,2-dichlorobenzene- d_4): δ 8.05 (d, $J = 6.9$ Hz, 2H, *o*-Ph), 7.42 (*pseudo*-t, 2H, *m*-Ph), 7.38 (d, $J = 7.6$ Hz, 2H, *o*-Ph), 7.23–7.20 (m, 3H, overlapped with 1,2-dichlorobenzene- d_3), 7.07–7.04 (m, 1H, overlapped with ^{13}C satellite of 1,2-dichlorobenzene- d_3). ^7Li NMR (155 MHz, 1,2-dichlorobenzene- d_4): δ -10.6 (s). ^{13}C NMR (151 MHz, 1,2-dichlorobenzene- d_4): 146.1, 145.2, 144.7, 144.1, 143.9, 143.9, 143.8, 143.6, 143.6, 143.4, 143.2, 142.7, 142.7, 142.6, 142.5, 142.1, 142.0, 141.9, 141.6, 140.7, 140.6, 140.5, 139.7, 139.6, 139.4, 138.8, 138.5, 138.2, 138.0, 137.0, 137.0, 136.6, 65.2, carbon peaks of the Ph group were overlapped with those of 1,2-dichlorobenzene- d_4 . High-resolution MALDI-FT-ICR MS (+): m/z calcd for $C_{73}\text{LiH}_{10}$ (M^+), 893.09371; found, 893.09357.

Procedures for the Synthesis of [6,6]- $[\text{Li}^+@C_{60}\text{Ph}_2]\text{TFSI}^-$. In a Schlenk tube, 1,2-dichlorobenzene (1.0 mL) solution of the mixture of [5,6]- and [6,6]- $[\text{Li}^+@C_{61}\text{Ph}_2]\text{TFSI}^-$ (4.5 mg, 3.8 μmol) was stirred at 160 °C under Ar atmosphere. After 3.5 h, the solution was concentrated in vacuo to ~0.4 mL and filtered. Recrystallization by vapor diffusion of diethyl ether afforded [6,6]- $[\text{Li}^+@C_{61}\text{Ph}_2]\text{TFSI}^-$ (3.8 mg, 84% yield). ^1H NMR (600 MHz, 1,2-dichlorobenzene- d_4): δ 8.12 (d, $J = 6.9$ Hz, 4H, *o*-Ph), 7.44 (*pseudo*-t, 4H, *m*-Ph), 7.38 (t, $J = 7.6$ Hz, 2H, *p*-Ph). ^7Li NMR (155 MHz, 1,2-dichlorobenzene- d_4): δ -12.4 (s). ^{13}C NMR (151 MHz, 1,2-dichlorobenzene- d_4): 146.7, 144.3, 144.1, 143.7, 143.7, 143.4, 143.1, 142.4, 142.3, 142.1, 142.1, 141.0, 140.5, 140.2, 137.0, 136.9, 80.8, 61.0, carbon peaks of the Ph group were overlapped with those of 1,2-dichlorobenzene- d_4 . High-resolution MALDI-FT-ICR MS (+): m/z calcd for $C_{73}\text{LiH}_{10}$ (M^+), 893.09371; found, 893.09363.

X-ray Structure Analysis. Single crystals of [5,6]- and [6,6]- $[\text{Li}^+@C_{61}\text{Ph}_2]\text{TFSI}^-$ were obtained by recrystallization from a chlorobenzene/diethyl ether solution and an *o*-dichlorobenzene/diethyl ether solution, respectively. X-ray diffraction measurements at 100 K were performed by using a large cylindrical image-plate camera at SPring-8 BL02B1. The programs SIR and SHELX were used for crystal structure analyses. The results are summarized in Table S3. The [5,6]- and [6,6]- $[\text{Li}^+@C_{61}\text{Ph}_2]\text{TFSI}^-$ crystals contain disordered chlorobenzene and *o*-dichlorobenzene solvent molecules, respectively. Both crystals have a similar molecular packing structure as shown in Figure S9. However, the crystal symmetries are different. The crystal symmetry of $P\bar{1}$ for the [5,6]-isomer with C_s symmetry is lower than that of $C2/m$ for the [6,6]-isomer with C_{2v} symmetry. Interestingly, disordered structures of C_{60} and TFSI $^-$ are also different. C_{60} and TFSI $^-$ are disordered and ordered, respectively, in the crystal of the [5,6]-isomer, whereas they are ordered and disordered, respectively, in

the crystal of the [6,6]-isomer. The disordered C₆₀ cage in the crystal of [5,6]-isomer has two orientations by 180° rotation around the axis through the cage center and the central carbon atom of the attached CPh₂ group. The refined site occupancies for the two orientations are 0.52 and 0.48. The ORTEP figures and bond lengths around the central carbon atom of the attached CPh₂ group for the major [5,6]-isomer and that of the [6,6]-isomer are shown in Figure S10.

■ ASSOCIATED CONTENT

Supporting Information

The Supporting Information is available free of charge on the ACS Publications website at DOI: 10.1021/acs.joc.7b00730.

X-ray crystal structure data (CIF)

X-ray crystal structure data (CIF)

Preparative HPLC charts, mass spectra, ¹H, ¹³C, and ⁷Li NMR spectra, UV-vis spectra, cyclic voltammograms (PDF)

■ AUTHOR INFORMATION

Corresponding Authors

*E-mail: aoyagi@nsc.nagoya-cu.ac.jp.

*E-mail: matsuo@photon.t.u-tokyo.ac.jp.

ORCID

Shinobu Aoyagi: 0000-0002-7393-343X

Yutaka Matsuo: 0000-0001-9084-9670

Notes

The authors declare no competing financial interest.

■ ACKNOWLEDGMENTS

This work was supported by the Grants-in-Aid for Scientific Research (JSPS KAKENHI grant nos. JP15H05760, JP16H04187, and JP17K04970) from the Ministry of Education, Culture, Sports, Science and Technology (MEXT), Japan. This work is also based on results obtained from a project commissioned by the New Energy and Industrial Technology Development Organization (NEDO), Japan. The HR-MS measurement was supported by “Nanotechnology Platform” of MEXT, Japan, at the Center for Integrated Nanotechnology Support, Tohoku University. The synchrotron radiation experiments were performed at SPring-8 with the approval of the Japan Synchrotron Radiation Research Institute (JASRI) (proposal no. 2014B0100).

■ REFERENCES

- (1) (a) Suzuki, T.; Li, Q.; Khemani, K. C.; Wudl, F.; Almarsson, Ö. *Science* **1991**, *254*, 1186–1188. (b) Suzuki, T.; Li, Q.; Khemani, K. C.; Wudl, F. *J. Am. Chem. Soc.* **1992**, *114*, 7301–7302.
- (2) Vasella, A.; Uhlmann, P.; Waldraff, C. A. A.; Diederich, F.; Thilgen, C. *Angew. Chem., Int. Ed. Engl.* **1992**, *31*, 1388–1390.
- (3) (a) Smith, A. B., III; Strongin, R. M.; Brard, L.; Furst, G. T.; Romanow, W. J.; Owens, K. G.; King, R. C. *J. Am. Chem. Soc.* **1993**, *115*, 5829–5830. (b) Smith, A. B., III; Strongin, R. M.; Brard, L.; Furst, G. T.; Romanow, W. J.; Owens, K. G.; Goldschmidt, R. J.; King, R. C. *J. Am. Chem. Soc.* **1995**, *117*, 5492–5502.
- (4) Prato, M.; Lucchini, V.; Maggini, M.; Stimpfl, E.; Scorrano, G.; Eiermann, M.; Suzuki, T.; Wudl, F. *J. Am. Chem. Soc.* **1993**, *115*, 8479–8480.
- (5) Diederich, F.; Isaacs, L.; Philp, D. J. *Chem. Soc., Perkin Trans. 2* **1994**, 391–394.
- (6) Osterodt, J.; Nieger, M.; Vogtle, F. *J. Chem. Soc., Chem. Commun.* **1994**, 1607–1608.
- (7) Hummelen, J. C.; Knight, B. W.; LePeg, F.; Wudl, F.; Yao, J.; Wilkins, C. L. *J. Org. Chem.* **1995**, *60*, 532–538.
- (8) Yu, G.; Gao, J.; Hummelen, J. C.; Wudl, F.; Heeger, A. J. *Science* **1995**, *270*, 1789–1791.
- (9) (a) Matsuo, Y.; Kawai, J.; Inada, H.; Nakagawa, T.; Ota, H.; Otsubo, S.; Nakamura, E. *Adv. Mater.* **2013**, *25*, 6266–6269. (b) Ryan, J. W.; Matsuo, Y. *Sci. Rep.* **2015**, *5*, 8319.
- (10) Xue, Q.; Bai, Y.; Liu, M.; Xia, R.; Chen, Z.; Hu, Z.; Jiang, X.-F.; Huang, F.; Yang, S.; Matsuo, Y.; Yip, H.-L.; Cao, Y. *Adv. Energy Mater.* **2017**, *7*, 1602333.
- (11) Iversen, B. B.; Darovsky, A.; Coppens, P. *Acta Crystallogr., Sect. B: Struct. Sci.* **1998**, *54*, 174–179.
- (12) (a) Aoyagi, S.; Nishibori, E.; Sawa, H.; Sugimoto, K.; Takata, M.; Miyata, Y.; Litauro, R.; Shinohara, H.; Okada, H.; Sakai, T.; Ono, Y.; Kawachi, K.; Yokoo, K.; Ono, S.; Omote, K.; Kasama, Y.; Ishikawa, S.; Komuro, T.; Tobita, H. *Nat. Chem.* **2010**, *2*, 678–683. (b) Okada, H.; Komuro, T.; Sakai, T.; Matsuo, Y.; Ono, Y.; Omote, K.; Yokoo, K.; Kawachi, K.; Kasama, Y.; Ono, S.; Hatakeyama, R.; Kaneko, T.; Tobita, H. *RSC Adv.* **2012**, *2*, 10624–10631. (c) Aoyagi, S.; Sado, Y.; Nishibori, E.; Sawa, H.; Okada, H.; Tobita, H.; Kasama, Y.; Kitaura, R.; Shinohara, H. *Angew. Chem., Int. Ed.* **2012**, *51*, 3377–3381.
- (13) (a) Ohkubo, K.; Kawashima, Y.; Fukuzumi, S. *Chem. Commun.* **2012**, *48*, 4314–4316. (b) Ohkubo, K.; Kawashima, Y.; Sakai, H.; Hasobe, T.; Fukuzumi, S. *Chem. Commun.* **2013**, *49*, 4474–4476. (c) Kawashima, Y.; Ohkubo, K.; Okada, H.; Matsuo, Y.; Fukuzumi, S. *ChemPhysChem* **2014**, *15*, 3782–3790. (d) Kawashima, Y.; Ohkubo, K.; Fukuzumi, S. *Chem. - Asian J.* **2015**, *10*, 44–54.
- (14) (a) Fukuzumi, S.; Ohkubo, K.; Kawashima, Y.; Kim, D. S.; Park, J. S.; Jana, A.; Lynch, V. M.; Kim, D.; Sessler, J. L. *J. Am. Chem. Soc.* **2011**, *133*, 15938–15941. (b) Davis, C. M.; Ohkubo, K.; Lammer, A. D.; Kim, D. S.; Kawashima, Y.; Sessler, J. L.; Fukuzumi, S. *Chem. Commun.* **2015**, *51*, 9789–9792.
- (15) (a) Aoyagi, S.; Tokumitsu, A.; Sugimoto, K.; Okada, H.; Hoshino, N.; Akutagawa, T. *J. Phys. Soc. Jpn.* **2016**, *85*, 094605. (b) Suzuki, H.; Ishida, M.; Yamashita, M.; Otani, C.; Kawachi, K.; Kasama, Y.; Kwon, E. *Phys. Chem. Chem. Phys.* **2016**, *18*, 31384–31387.
- (16) (a) Matsuo, Y.; Okada, H.; Maruyama, M.; Sato, H.; Tobita, H.; Ono, Y.; Omote, K.; Kawachi, K.; Kasama, Y. *Org. Lett.* **2012**, *14*, 3784–3787. (b) Kawakami, H.; Okada, H.; Matsuo, Y. *Org. Lett.* **2013**, *15*, 4466–4469. (c) Ueno, H.; Kawakami, H.; Nakagawa, K.; Okada, H.; Ikuma, N.; Aoyagi, S.; Kokubo, K.; Matsuo, Y.; Oshima, T. *J. Am. Chem. Soc.* **2014**, *136*, 11162–11167. (d) Watanabe, T.; Itoh, M. F.; Komuro, T.; Okada, H.; Sakai, T.; Ono, Y.; Kawachi, K.; Kasama, Y.; Tobita, H. *Organometallics* **2014**, *33*, 608–611. (e) Ueno, H.; Aoyagi, S.; Yamazaki, Y.; Ohkubo, K.; Ikuma, N.; Okada, H.; Kato, T.; Matsuo, Y.; Fukuzumi, S.; Kokubo, K. *Chem. Sci.* **2016**, *7*, 5770–5774.
- (17) Okada, H.; Matsuo, Y. *Fullerenes, Nanotubes, Carbon Nanostruct.* **2014**, *22*, 262–268.
- (18) Oshima, T.; Kitamura, H.; Higashi, T.; Kokubo, K.; Seike, N. *J. Org. Chem.* **2006**, *71*, 2995–3000.
- (19) (a) Komatsu, K.; Murata, M.; Murata, Y. *Science* **2005**, *307*, 238–240. (b) Murata, M.; Murata, Y.; Komatsu, K. *J. Am. Chem. Soc.* **2006**, *128*, 8024–8033.
- (20) Chen, Z.; Cioslowski, J.; Rao, N.; Moncrieff, D.; Bühl, M.; Hirsch, A.; Thiel, W. *Theor. Chem. Acc.* **2001**, *106*, 364–368.
- (21) (a) Kiely, A. F.; Haddon, R. C.; Meier, M. S.; Selegue, J. P.; Brock, C. P.; Patrick, B. O.; Wang, G.-W.; Chen, Y. *J. Am. Chem. Soc.* **1999**, *121*, 7971–7972. (b) Lu, X.; Nikawa, H.; Tsuchiya, T.; Maeda, Y.; Ishitsuka, M. O.; Akasaka, T.; Toki, M.; Sawa, H.; Slanina, Z.; Mizorogi, N.; Nagase, S. *Angew. Chem., Int. Ed.* **2008**, *47*, 8642–8645.
- (22) (a) Janssen, R. A. J.; Hummelen, J. C.; Wudl, F. *J. Am. Chem. Soc.* **1995**, *117*, 544–545. (b) Gonzalez, R.; Hummelen, J. C.; Wudl, F. *J. Org. Chem.* **1995**, *60*, 2618–2620.
- (23) (a) Hirsch, A.; Brettreich, M. *Fullerenes: Chemistry and Reactions*; Wiley-VCH: Weinheim, Germany, 2015. (b) Thilgen, C.; Diederich, F. *Chem. Rev.* **2006**, *106*, 5049–5135.
- (24) Schroeder, W.; Katz, L. *J. Org. Chem.* **1954**, *19*, 718–720.